

RESEARCH ACTIVITIES V

Department of Applied Molecular Science

V-A Magnetic Structure of Oligo-Nitroxide-Transition Metal Complexes

Since one or two decades, considerable attention has been devoted to stable nitroxide radicals and their metal complexes which are now widely used as building blocks for the design of molecular-based magnetic materials. In this field, we have introduced a new strategy of employing π -conjugated polyaminoxyls as ligands in which the 2p-spins of the NO groups interact ferromagnetically ($J_1 > 0$). The dimensionality of the complex and the sign and magnitude of the exchange coupling between the neighboring spins may be readily tuned by this strategy. Depending on the nature of the additional interchain or interlayer interaction, the polymers are expected to become an antiferromagnet or ferri/ferromagnet. By modifying and extending this design strategy to bis- and tris(aminoxyl) radicals having triplet and quartet ground states, respectively, we have been able to construct with the aid of magnetic metal ions one-dimensional (1D) chain, two-dimensional (2D) network and three-dimensional (3D) parallel-crosses structures in which both the organic 2p and metallic 3d spins have been ordered in macroscopic scales. Since such a rational approach by self-assembly to the tailored extended systems having relevant physical properties is of great importance in materials synthesis. For these materials, the magnetic structures of the crystals are also interesting.

V-A-1 Magnetic Properties of Layered Complexes $[M(\text{hfac})_2]_3 \cdot (\text{R})_2$, $M = \text{Mn(II)}$ and Cu(II) , with Trisnitroxide Radicals Having Various Metal-Radical Exchange Interactions

TANAKA, Motoko; HOSOKOSHI, Yuko;
MARKOSYAN, Ashot S.¹; IWAMURA, Hiizu²;
INOUE, Katsuya

(¹IMS and M.V. Lomonosov Moscow State Univ.;
²Kyushu Univ.)

[*J. Phys.: Condens. Matter* **13**, 7429 (2001)]

A series of new layered 2D-network complexes $[M(\text{hfac})_2]_3(\text{R}_\Delta)_2$ of $M = \text{Mn(II)}$ and Cu(II) with trisnitroxide radicals R_Δ has been prepared and the magnetic properties were studied. Each triradical R_Δ has a quartet ground state and contributes not only to the formation of extended structures but essentially to the overall magnetism. Several exchange interactions, between M and nitroxide, intraradical nitroxide–nitroxide interactions, are responsible for the development of the characteristic magnetic properties in these heterospin systems. Depending on the nature of the interlayer interactions, they show either ferro/ferrimagnetic or antiferromagnetic long range order. The hierarchy of the different exchange interactions is established and the Mn–nitroxide and Cu–nitroxide exchange integrals are evaluated from the analysis of the temperature dependence of the paramagnetic susceptibility. With increasing intraradical exchange interaction, the complexes exhibit more pronounced 2D behavior.

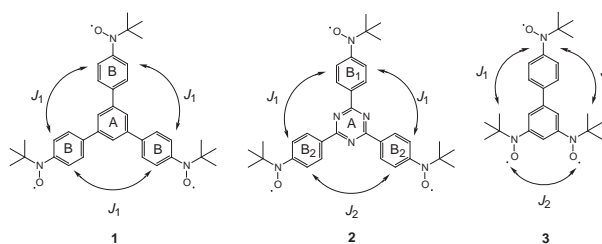


Figure 1. Triangular triradicals **1** ($J_1/k_B = 6.8$ K), **2** ($J_1/k_B = 15.3$ K, $J_2/k_B = 11.8$ K) and **3** ($J_1/k_B \approx 67$ K, $J_2/k_B > 200$ K) with three ligating sites, where A and B indicate the aromatic rings in different positions. J_1/k_B and J_2/k_B were found for the crystals of **1** and **2** or for isolated molecules of **3**. Only the radical **1** has threefold symmetry.

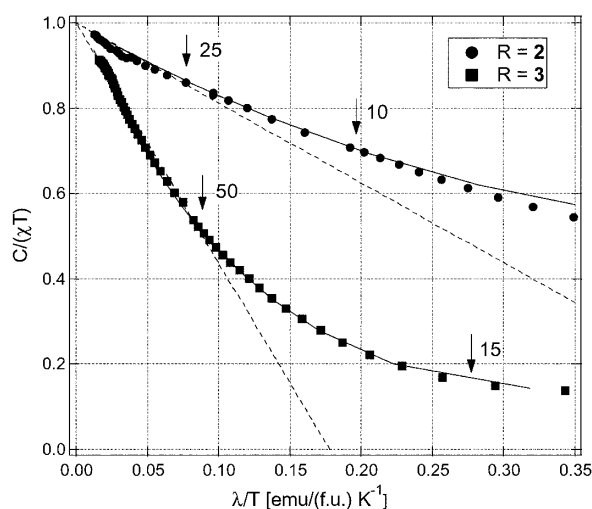


Figure 2. $C/(\chi T)$ vs. λ/T plots for $[\text{Mn}(\text{hfac})_2]_3(\mathbf{2})_2 \cdot (\text{C}_6\text{H}_6)_3$ and $[\text{Mn}(\text{hfac})_2]_3(\mathbf{3})_2$. The solid and dot lines show the behavior for the 2D and 3D models, respectively. Some temperatures are indicated by arrows for clarity.

V-B Synthesis of Chiral Molecule-Based Magnets

The design of molecular materials with interesting magnetic and optical or electrical properties is one of the major challenges in the last few years. The synthesis and study of chiral molecular-based magnetic materials which are transparent for light are of great interest. Novel magneto-optical phenomena have been theoretically predicted and observed in chiral paramagnetic materials in 1997. Although novel properties are expected for such compounds, few examples of chiral molecular-based magnetic materials are still known. To get more insight in their properties it is therefore important to construct such chiral molecule-based magnets in a systematic way. We designed and synthesized a chiral organic radical which can be employed to construct chiral molecular-based magnets.

V-B-1 Synthesis and Structure of Chiral Molecule-Based Three-Dimensional Ferrimagnet

INOUE, Katsuya; IMAI, Hiroyuki; GHALSASI, Prasanna S.¹; KIKUCHI, Koichi²; OHBA, Masaaki³; OKAWA, Hisashi³; YAKHMI, J. V.⁴
 (¹IMS and Univ. Mumbai; ²Tokyo Metropolitan Univ.; ³Kyusyu Univ.; ⁴Bhabha Atomic Res. Cent.)

New chiral, transparent, high $T_C = 53$ K molecule-based three-dimensional ferrimagnet, $K_{0.4}[Cr(CN)_6][Mn(S)\text{-pn}](S)\text{-pn}H_{0.6}$; ((*S*)-pn = (*S*)-1,2-diaminopropane) are synthesized. The complex was obtained as pale yellow needle crystal by the reaction of $K_3[Cr(CN)_6]$, $Mn(ClO_4)_2$, and (*S*)-1,2-diaminopropane dihydrochloride ((*S*)-pn·2HCl). X-ray structural analysis revealed a crystallized chiral space group of hexagonal $P6_1$; moreover, the complex demonstrated a three-dimensional magnetic network. (Figure 1) The magnetic measurements of the complex show Mn^{II} and Cr^{III} ions interact ferrimagnetically and magnetic transition occurs at 53 K.



Figure 1. Crystal structure of $K_{0.4}[Cr(CN)_6][Mn(S)\text{-pn}](S)\text{-pn}H_{0.6}$. View along the *c* axis and showing the connection of helical dimetallic loops.

V-C Synthesis and Characterization of Quantum-Spin Systems

There has been considerable current interest in the study of a low-dimensional quantum-spin system with an energy gap. For such study, organic radicals will provide good examples of ideal Heisenberg spin systems, since they consist only of light elements. By the appropriate design of molecules, we can obtain a variety of spin systems. In these years, we focus on the spin-ladder system, which is interesting in terms of Haldane state and the high T_C superconductivity. For the $S = 1/2$ Heisenberg spin ladder with antiferromagnetic legs and rungs, the ground state of the resonating valence bond (RVB) state or the dimerized state is theoretically expected. Experimentally, the singlet ground state was observed in some ladder systems formed by Cu-based compounds. The study of spin ladder systems has been mainly devoted to that of $S = 1/2$, but that of $S = 1$ is also interesting. For the ground state of the $S = 1$ ladder with antiferromagnetic legs ($J_{||}$) and rungs (J_{\perp}), the Haldane state is expected in the extreme limit of $J_{\perp} \rightarrow 0$, and the dimer state in $J_{||} \rightarrow 0$. In its ground state phase diagram on the $J_{||}/J_{\perp}$ versus the energy gap (Δ), the phase transition from the dimer state to the Haldane state through a gapless point can be expected. A similar behavior of an existence of a gapless point between two different phases with their own finite excitation gaps is known for the $S = 1$ Heisenberg alternating antiferromagnetic chain system.

V-C-1 Magnetic Properties of Organic Spin Ladder Systems

HOSOKOSHI, Yuko; KATO, Keiichi¹;
MARKOSYAN, Ashot S.²; INOUE, Katsuya
(¹GUAS; ²IMS and M.V. Lomonosov Moscow State Univ.)

[*Synth. Met.* **121**, 1939 (2001)]

Novel organic polyradicals, BIP-BNO and BIP-TENO, are synthesized and crystallized to form ladder systems, where BIP-BNO and BIP-TENO denote 3,5'-bis(*N*-*tert*-butylaminoxyl)-3',5'-dibromobiphenyl and 3,3',5,5'-tetrakis(*N*-*tert*-butylaminoxyl)biphenyl, respectively. The BIP-BNO crystals form a two-leg ladder of $S = 1/2$ with antiferromagnetic legs and rungs. The BIP-TENO crystals can be regarded as a two-leg ladder of $S = 1$ species. The magnetic measurements revealed that both compound have singlet ground states.

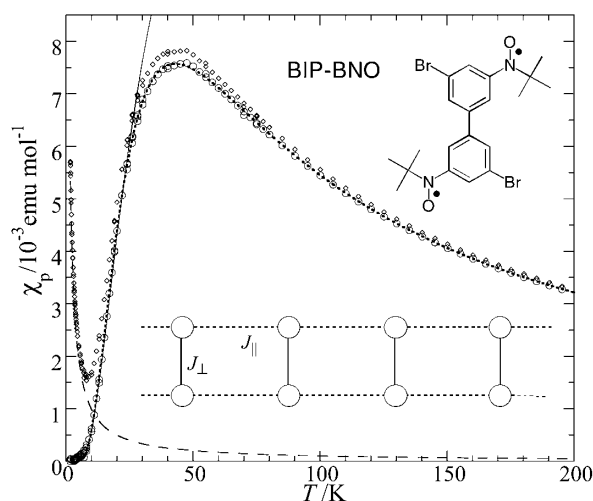


Figure 1. Temperature dependence of the paramagnetic susceptibility (χ_p) of BIP-BNO. Observed data are represented by diamonds (\diamond). Open circles represent data after the subtraction of the Curie impurity (broken curve). The dotted curve is the calculation for the ladder system (12 spins) with $2J_{\perp}/k_B = -66.4$ K and $2J_{\parallel}/k_B = -26$ K. The solid curve is the fit of $\chi \propto \exp(\Delta/T)/T$ with $\Delta = 47$ K.

V-C-2 Observation of Magnetization Plateau of 1/4 in a Novel Double Spin Chain of Ferromagnetic Dimers formed by an Organic Tetraradical

GOTO, Tsuneaki¹; BARTASHEVICH, M. I.¹;
HOSOKOSHI, Yuko; KATO, Keiichi²; INOUE, Katsuya
(¹ISSP, Univ. of Tokyo; ²GUAS)

[*Physica B* **294**, 43 (2001)]

We have measured the susceptibility and low temperature magnetization curve of the novel organic tetraradical crystal BIP-TENO. The susceptibility data indicate that double spin chains of ferromagnetic dimers are formed in the crystal and the spin system is regarded as an $S = 1$ antiferromagnetic two-leg ladder. The magnetization is nearly zero up to 10 T and the spin gap is closed at 11.6 T. Above 12 T, the magnetization increases and a plateau corresponding to a quarter of the saturation magnetization appears at 44.8 T.

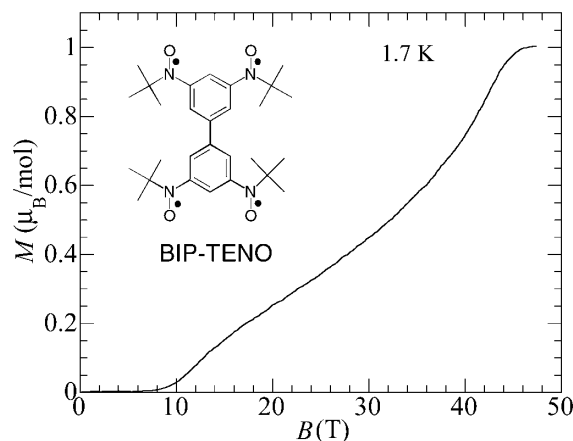


Figure 1. Magnetization curve of BIP-TENO at 1.7 K in pulsed high magnetic fields up to about 50 T.

V-D Organic Ferrimagnetism

In the last decades, the magnetism of molecule-based material has drawn much interest. After the discovery of the organic ferromagnet in 1991, search for an organic ferrimagnet attracts great interest and is considered as one of today's challenging targets in material science. Although a number of ferrimagnets are realized in inorganic-organic hybrid systems, a genuine organic ferrimagnet has not yet been realized. In 1980's, ferrimagnetism is proposed as an effective strategy to give organic materials spontaneous magnetizations by the alternant arrangement of two kinds of organic radicals having different spin-multiplicities. All the reported ferrimagnets include at least two magnetic components: bimetallic compounds or metal complexes with organic radicals. In order to achieve this challenging subject of an organic ferrimagnet from a different viewpoint, we propose here a single-component strategy: utilizing a triradical including an $S = 1$ and an $S = 1/2$ units within a molecule and connecting the $S = 1$ and $S = 1/2$ units by intra- and intermolecular antiferromagnetic interactions. Our new strategy to use a single component has the advantages of the easiness of controlling the crystal structure and the good crystallinity for quality and size.

V-D-1 Approach to a Single-Component Ferrimagnetism by Organic Radical Crystals

HOSOKOSHI, Yuko; KATO, Keiichi¹;
NAKAZAWA, Yasuhiro²; NAKANO, Hiroki³;
INOUE, Katsuya
(¹GUAS; ²Osaka Univ.; ³Univ. Tokyo)

[*J. Am. Chem. Soc.* **123**, 7921 (2001)]

A novel organic triradical of 2-[3',5'-bis(*N*-tert-butylaminoxyl)phenyl]-4,4,5,5-tetramethyl-4,5-dihydro-1*H*-imidazol-1-oxyl 3-oxide, abbreviated as PNNBNO, were synthesized. The PNNBNO molecule includes three $S = 1/2$ spins and is regarded as the antiferromagnetic pair of an $S = 1/2$ and $S = 1$. In the crystals, the planar PNNBNO molecules stack along the b axis forming the alternant array of the $S = 1/2$ and the $S = 1$. This can be regarded as a ferrimagnetic ladder, with rungs of intramolecular antiferromagnetic interactions and legs of intermolecular antiferromagnetic interactions between the $S = 1/2$ and $S = 1$. In the static magnetic susceptibility measurements, clear ferrimagnetic behavior is observed. Moreover, we must mention that the crystals include the 3D ferrimagnetic

network. Each ladder is surrounded by four neighboring ladders with the alternant alignment of the $S = 1/2$ and $S = 1$. The heat capacity measurements revealed that the effective $S = 1/2$ species (ferrimagnetic spins) undergo a magnetic phase transition at 0.28 K. This is the first example of a genuine organic ferrimagnetic material having well-defined chemical and crystal structure.

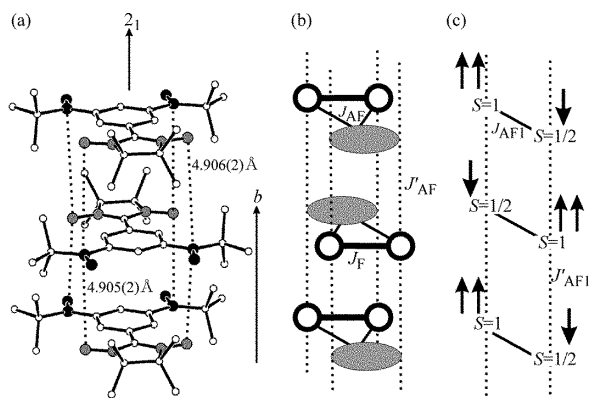


Figure 1. (a) Uniform chain structure in PNNBNO crystals. (b) Schematic illustration of the chain structure. (c) Ferrimagnetic ladder structure in the extreme limit when $J_F \rightarrow \infty$.

V-E Pressure Effects on Molecular Magnetism

'Pressure' is a powerful tool to control the molecular packings and physical properties. The molecule-based materials with small densities are 'soft' and can be expected to show large pressure effects. For the magnetic measurements with high-accuracy, we have developed a small high-pressure clamp cell made of non-magnetic Cu-Ti alloy which can be equipped to a Quantum Design SQUID magnetometer for the dc and ac magnetic measurements. The inner pressure of the clamp cell has been calibrated by the superconducting transition temperature of Pb. We have already discovered that some kind of structural change can be suppressed by pressurization. We are now studying the pressure effects on the molecule-based magnetic materials in wider range. In molecular materials, the spin density are delocalized and distributed in a molecule and the spin-density-distribution plays an important role in the exchange interactions. It is attractive to control the sign of the exchange coupling by pressurization. The pressure effects on the related compounds with similar crystal structures are studied.

V-E-1 Pressure Effect on Mn Complexes of Bisaminoxyl Radicals

HOSOKOSHI, Yuko; SUZUKI, Kentaro¹; INOUE, Katsuya
(¹GUAS)

The pressure effects on the magnetic properties of one-dimensional Mn(hfac)₂ complexes with 1,3-bis(*N*-tert-butylaminoxyl)benzene (**1_H**) and 5-halo-1,3-bis(*N*-tert-butylaminoxyl)benzene (**1_F**, **1_{Cl}**, **1_{Br}**) have been studied. These complexes have similar chain structures and undergo three-dimensional magnetic phase transitions at low temperature, due to weak interchain interactions. At ambient pressure, **1_H** and **1_F** are metamagnets with weak interchain antiferromagnetic interactions, whereas **1_{Cl}** and **1_{Br}** are ferrimagnets with weak interchain ferromagnetic interactions. The opposite sign of the interchain interactions in these materials is attributed to the different way of packing

between the chains. The pressurization of the both metamagnets, results in the monotonous increase of the interchain antiferromagnetic interactions. The enhancement of T_N and H_C with applying pressure was observed. On the other hand, the both ferrimagnets show curious pressure dependences. The change of the interchain interaction is very sensitive to pressure. In some pressure region, temperature dependence of the ac susceptibility shows two peaks. One of the peaks is readily broadened in the existence of the small external DC field of 5–25 Oe. The mechanism of the interchain interaction is discussed.

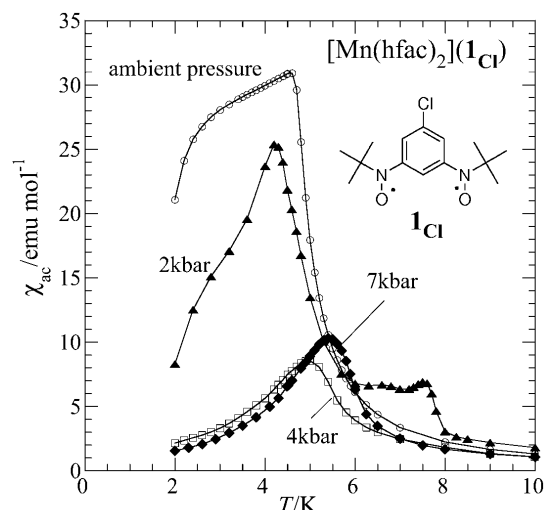


Figure 1. Temperature dependence of the ac susceptibility of $[\text{Mn}(\text{hfac})_2] \cdot 1_{\text{Cl}}$ under several pressures.

V-E-2 Suppression of the Structural Change under Pressure of $\text{Cu}(\text{hfac})_2$ Complex with 5-Bromo-1,3-phenylenebis(*N*-*tert*-butyl-aminoxyl)

HOSOKOSHI, Yuko; SUZUKI, Kentaro¹;
IWAHORI, Fumiyasu¹; INOUE, Katsuya
(¹GUAS)

The pressure effect on the magnetic properties of 3:2 complex of $\text{Cu}(\text{hfac})_2$ with 5-Bromo-1,3-phenylenebis(*N*-*tert*-butyl-aminoxyl) (1_{Br}) has been studied. At ambient pressure, sudden decrease of magnetic susceptibility at 48 K was reported, which suggests the structural change at this temperature. Our magnetic measurements under pressure revealed that the structural change is sufficiently suppressed at 6 kbar. We also found that the weak stress when the sample is dipped in oil, affects the structural change. The behavior suggests that, at 6 kbar, the high-temperature phase is preserved down to low temperature as metastable state. The enhancement of the energy barrier of the structural transition under pressure is suggested.

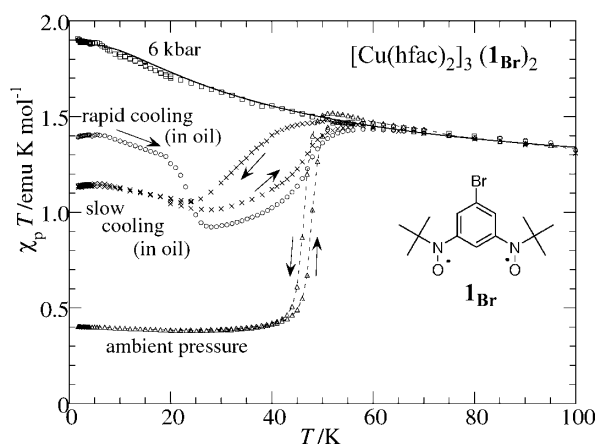


Figure 1. Temperature dependence of $\chi_p T$ of $[\text{Cu}(\text{hfac})_2]_3 \cdot (1_{\text{Br}})_2$ at ambient pressure (Δ), at 6 kbar (\square), and in oil (\circ , \times).

V-F Bioinorganic Studies on Structures and Functions of Non-heme Metalloenzymes Using Model Complexes

Metal-containing enzymes have been widely distributed in both plants and animals and have been related to metabolic processes such as hydroxylation, oxygen transport, oxidative catalysis, electron transfer, and so on. In this project the structures and functions for the metal complexes are studied as a model of several metallo-enzymes by using some physico-chemical methods.

V-F-1 Electron Transfer Reaction Induced by Self-Assembly of Biguanidato and Violurato Complexes through Triple Hydrogen-Bond

KITAMURA, Hideki¹; OZAWA, Tomohiro¹;
JITSUKAWA, Koichiro¹; MASUDA, Hideki²;
EINAGA, Hisahiko¹

(¹Nagoya Inst. Tech.; ²IMS and Nagoya Inst. Tech.)

[*Kobunshi Ronbunshu* **57**, 188 (2000)]

Hydrogen bond, which is one of the non-covalent interactions, plays an important role for controlling supramolecular synthesis through metal-induced self-assembly of organic compounds as well as covalent- and coordinate-bonds. The 1:1 mixture of [Co(bg)₃] and [Co(va)₃] complexes containing biguanidato (bg) and violuric acid (va) ligands, which enable formation of ADA-DAD style hydrogen bonding, respectively, gave a three-dimensional network structure constructed with triple hydrogen bonding interaction accompanying interligand proton transfer equilibrium. Internal void in this structure formed by the aggregation of the polar functions of bg and va may capture water molecule through the bonding. Moreover, an interesting electron transfer reaction, Cu(II) + Mn(III) → Cu(I) + Mn(IV), was observed in the 1:1 mixture system consisting of square planar [Cu(va)₂] and octahedral [Mn(enbg)(OH)(H₂O)] complexes, when the linear tape structure was generated through the interligand hydrogen bonding between va ligand and ethylenebisbiguanidato (enbg). Oxidation of Mn(III) to Mn(IV) by Cu(II) supported by the reduction potential of the complexes might be occurred through the bonding of Mn-O-Cu, which was accurately generated by the two-dimensional assembly of this linear tape.

V-F-2 A Novel Diiron Complex as a Functional Model for Hemerythrin

ARII, Hidekazu¹; NAGATOMO, Shigenori;
KITAGAWA, Teizo; MIWA, Tomohiro¹;
JITSUKAWA, Koichiro¹; EINAGA, Hisahiko¹;
MASUDA, Hideki²

(¹Nagoya Inst. Tech.; ²IMS and Nagoya Inst. Tech.)

[*J. Inorg. Biochem.* **82**, 153 (2000)]

Diiron(II) complexes with a novel dinucleating polypyridine ligand, *N,N,N',N'*-tetrakis(6-pivalamido-2-pyridylmethyl)-1,3-diaminopropan-2-ol (HTPPDO), were synthesized as functional models of hemerythrin. Structural characterization of the complexes, [Fe^{II}₂-

(Htppdo)(PhCOO)](ClO₄)₃ (**1**), [Fe^{II}₂(Htppdo)(*p*-Cl-PhCOO)](ClO₄)₃ (**2**), [Fe^{II}₂(Htppdo)(*p*-Cl-PhCOO)](BF₄)₃ (**2'**) and [Fe^{II}₂(tppdo)(*p*-Cl-PhCOO)](ClO₄)₂ (**3**), were accomplished by electronic absorption, and IR spectroscopic, electrochemical, and X-ray diffraction methods. The crystal structures of **1** and **2'** revealed that the two iron atoms are asymmetrically coordinated with HTPPDO and bridging benzoate. One of the iron centers (Fe(1)) has a seven-coordinate capped octahedral geometry comprised of an N₃O₄ donor set which includes the propanol oxygen of HTPPDO. The other iron center (Fe(2)) forms an octahedron with an N₃O₃ donor set and one vacant site. The two iron atoms are bridged by benzoate (**1**) or *p*-chlorobenzoate (**2**). On the other hand, Fe atoms of complex **3** are both symmetrically coordinated with N₃O₄ donors and two bridging ligands; benzoate and the propanolate of TPPDO. Reactions of these complexes with dioxygen were followed by electronic absorption, resonance Raman and ESR spectroscopies. Reversible dioxygen-binding was demonstrated by observation of an intense LMCT band for O₂²⁻ to Fe(III) at 610 (**1**) and 606 nm (**2**) upon exposure of dioxygen to acetone solutions of **1** and **2** prepared under an anaerobic conditions at -50 °C. The resonance Raman spectra of the dioxygen adduct of **1** exhibited two peaks assignable to the ν(O-O) stretching mode at 873 and 887 cm⁻¹, which shifted to 825 and 839 cm⁻¹ upon binding of ¹⁸O₂. ESR spectra of all dioxygen adducts were silent. These findings suggest that dioxygen coordinates to the diiron atoms as a peroxo anion in a μ-1,2 mode. Complex **3** exhibited irreversible dioxygen binding. These results indicate that the reversible binding of dioxygen is governed by the hydrophobicity of the dioxygen-binding environment rather than the iron redox potentials.

V-F-3 A Substrate-specific α-Hydroxylation of Dipeptides Mediated upon a Co(III)-terpyridine Complex: A Functional Model for Peptidylglycine α-Hydroxylating Monooxygenase

JITSUKAWA, Koichiro¹; IRISA, Tsuyoshi¹;
EINAGA, Hisahiko¹; MASUDA, Hideki²

(¹Nagoya Inst. Tech.; ²IMS and Nagoya Inst. Tech.)

[*Chem. Lett.* **30** (2001)]

A substrate-specific α-hydroxylation of dipeptides has been found out as a functional model for peptidylglycine α-hydroxylating monooxygenase (PHM), in the reaction of the Co(III) ternary complexes containing terpyridine and dipeptide ligands under aerobic and slightly alkaline conditions.

V-F-4 Site-Selective Recognition of Amino Acids by Co(III) Complexes Containing a (N)(O)₃-Type Tripodal Tetradentate Ligand

KUMITA, Hideyuki¹; MORIOKA, Taiju¹; OZAWA, Tomohiro¹; JITSUKAWA, Koichiro¹; EINAGA, Hisahiko¹; MASUDA, Hideki²

(¹Nagoya Inst. Tech.; ²IMS and Nagoya Inst. Tech.)

[*Bull. Chem. Soc. Jpn.* **74**, 1035 (2001)]

The bis-*N,N*-carboxymethyl-(*S*)-phenylalaninato carbonato cobalt(III) complex, [Co(bcmpa)(CO₃)]²⁻, has been prepared as a simple model that enables the recognition of an amino acid (Haa) whose coordination behaviours in solution have been characterized by electronic absorption (AB), circular dichroism (CD) and ¹H-NMR spectroscopies. The reaction of the K₂[Co-(bcmpa)(CO₃)] complex with amino acids (Haa) has predominantly afforded the [Co(bcmpa)(aa)] complex in the *trans(N)*-configuration mode, rather than in the *cis(N)*-form. By using amino acid derivatives with bulky substituents at their amino or carboxylate sites under a neutral condition, the reactions have been demonstrated to be initiated by coordination of the amino nitrogen site. Interestingly, the *cis(N)*-complex, which is isolated as a minor product, isomerizes to the *trans(N)*-form in the presence of active charcoal under pH 7 in an aqueous solution. The site-selective coordination of Haa to the [Co(bcmpa)(CO₃)]²⁻ complex and the stereoselective isomerization of the [Co(bcmpa)(aa)]⁻ complex have been explained to be regulated by weak non-covalent interactions within the ligands, whose origin has been discussed based on a detailed examination of the crystal structures of the *trans(N)*- and *cis(N)*-K[Co(bcmpa)(aa)] complexes.

V-F-5 Crystal Structure and Redox Behavior of a Novel Siderophore Model System: A Trihydroxamate-iron(III) Complex with Intra- and Interstrand Hydrogen Bonding Networks

MATSUMOTO, Kenji¹; OZAWA, Tomohiro¹; JITSUKAWA, Koichiro¹; EINAGA, Hisahiko¹; MASUDA, Hideki²

(¹Nagoya Inst. Tech.; ²IMS and Nagoya Inst. Tech.)

[*Inorg. Chem.* **40**, 190 (2001)]

An iron(III) complex of a novel tripodal tris-hydroxamate with intramolecular hydrogen-bonding networks (**1**), tris[2-{(N-acetyl-N-hydroxy)glycyl-amino}ethyl]amine (TAHGA), has been synthesized as a siderophore model, whose crystal structure revealed the formation of the intra- and interstrand hydrogen bonding networks. Formation of the strong hydrogen bonding networks has also been demonstrated in a DMSO solution using the corresponding gallium(III) complex by ¹H-NMR spectroscopy. The amide proton peak of Ga(III)-TAHGA was quite independent on temperature in the range of 303–323 K, indicating that the amide hydrogens of the Ga(III)-TAHGA complex are well shielded from the outer sphere and are tightly protected from hydrolysis of the complex. The redox

behavior of **1** in an aqueous solution exhibited higher potential (–230 mV vs. NHE) for its larger pM value (25.1) compared with those for natural siderophores reported hitherto, indicating that the hydrogen-bonds with the coordinating aminohydroxyl oxygens cause to lower the potential of metal ion. It is suggested that the inter- and intrastrand hydrogen-bonding interactions play an important role for not only tight holding of the iron(III) atom and its shielding from the outer sphere but also control of the redox potential of the central metal ion.

V-F-6 Characterization of an NH-π Interaction in Co(III) Ternary Complexes with Aromatic Amino Acids

KUMITA, Hideyuki¹; JITSUKAWA, Koichiro¹; EINAGA, Hisahiko¹; MASUDA, Hideki²

(¹Nagoya Inst. Tech.; ²IMS and Nagoya Inst. Tech.)

[*Inorg. Chem.* **40**, 3936 (2001)]

The NH-π interaction has been detected in the crystal structures of Co(III) ternary complexes with *N,N*-bis(carboxymethyl)-(*S*)-phenylalanine (BCMPA) and aromatic amino acids including: (*S*)-phenylalanine ((*S*)-Phe), (*R*)-phenylalanine ((*R*)-Phe), and (*S*)-tryptophan ((*S*)-Trp). Additionally, this interaction has been characterized in solution for Co(III) ternary complexes with BCMPA or NTA (NTA = nitrilotriacetic acid) and several amino acids (AA) by means of electronic absorption, circular dichroism (CD), and ¹H NMR spectroscopies. The CD intensities of the Co(III) complexes with aromatic amino acids measured in the d-d region (~ 20.5 × 10³ cm⁻¹) are significantly decreased in ethanol solutions relative to water. Analogous complexes with aliphatic amino acids do not exhibit this solvent effect. The ¹H NMR spectra of the Co(III) complexes with aromatic amino acids in DMSO-d₆ exhibit up-field shifts of the N–H peaks compared with those with aliphatic amino acids, which suggest a shielding effect due to the aromaticity. The up-shift values coincide with those experimentally evaluated from the crystal structures. The magnitude in the upper field shifts agrees well with Hammett's rule, indicating that the increase of π-electron densities on the aromatic rings exerts a larger shielding effect for the NH protons. In ligand-substitution reactions of the carbonatocobalt(III) complexes with amino acids, the yields of those with aromatic amino acids are higher than the yields obtained for complexes with aliphatic amino acids. This observation is discussed in connection with the important contribution of the NH-π interaction as one of the promotion factors in the reaction.

V-F-7 Reverse Reactivity in Hydroxylation of Adamantane and Epoxidation of Cyclohexene Catalyzed by the Mononuclear Ruthenium-oxo Complexes with 6-Substituted Tripodal Polypyridine Ligands

JITSUKAWA, Koichiro¹; OKA, Yoshiyuki¹; EINAGA, Hisahiko¹; MASUDA, Hideki²

(¹Nagoya Inst. Tech.; ²IMS and Nagoya Inst. Tech.)

[*Tetrahedron Lett.* **42**, 3467 (2001)]

The electronic character of the ruthenium complexes with tripodal polypyridine ligands, which is controlled by the substituted groups at pyridine 6-position, gives rise to differences in the reactivity for the ruthenium catalyzed hydroxylation of adamantane and epoxidation of cyclohexene with PhIO as an oxidant; Ru complexes containing electron-withdrawing groups (**1**, **3**, and **5**) promote the epoxidation, while those containing electron-donating groups (**2**, **4**, and **6**) promote the hydroxylation.

V-F-8 A Structural Model of the Ferrichrome Type Siderophore: Chiral Preference Induced by Intramolecular Hydrogen Bonding Networks in Ferric Trihydroxamate

MATSUMOTO, Kenji¹; OZAWA, Tomohiro¹;
JITSUKAWA, Koichiro¹; EINAGA, Hisahiko¹;
MASUDA, Hideki²

(¹Nagoya Inst. Tech.; ²IMS and Nagoya Inst. Tech.)

[*Chem. Commun.* 978 (2001)]

Tris[2-(N-acetyl-N-hydroxy)-D-alanyl-amino]-ethylamine (*R*-TAAE) has been synthesized as a chiral trihydroxamate artificial siderophore with hydrogen bonding networks, whose crystal structure of the iron(III) complex revealed Λ configuration induced by interstrand hydrogen bonding networks and steric repulsion by optically active amino acid residues.

V-F-9 Crystal Structure and Solution Behavior of the Iron(III) Complex of the Artificial Trihydroxamate Siderophore with Tris(3-aminopropyl)amine Backbone

MATSUMOTO, Kenji¹; SUZUKI, Naomi¹;
OZAWA, Tomohiro¹; JITSUKAWA, Koichiro¹;
MASUDA, Hideki²

(¹Nagoya Inst. Tech.; ²IMS and Nagoya Inst. Tech.)

[*Eur. J. Inorg. Chem.* **10**, 2481 (2001)]

Microorganisms produce low molecular weight compounds called siderophores for an uptake of iron. The iron(III)-siderophore complexes are very stable and the ligand backbones as well as the iron(III)-binding groups are important for the stabilization of iron(III) complexes. Although many tripodal artificial siderophore analogues have been synthesized as ferrichrome and enterobactin analogues, tris(3-aminopropyl)amine (TRPN) has not been much employed as tripodal anchor and the details are little examined. Here, we report the synthesis of newly designed tris[3-(N-acetyl-N-hydroxy)-glycylamino]-propylamine (TAGP) as a trihydroxamate artificial siderophore with TRPN anchor and the crystal structure and solution behaviors of its iron(III) complex. The crystal structure of iron(III)-TAGP complex is the first report on the trihydroxamate artificial siderophore with TRPN anchor which is very similar to the calculated lowest energy conformation of the iron(III) complex of

the trihydroxamate with triscarboxylate anchor previously reported. However, the solution behaviors of these iron(III) complexes are quite different from. TAGP forms the 1:1 tris(hydroxamato)-iron(III) complex in pH 2–8, while, the ferrichrome analogue with triscarboxylate anchor forms polymeric and polynuclear iron(III) complexes, despite the higher conformational similarity between these iron(III) complexes. Interestingly, the former promotes the growth of the siderophore-auxotrophic bacterium, while the latter does not. These results suggest that the TRPN tripodal anchors are quite important not only for the stabilization of iron(III) complexes in strong acidic pH but also for the biological activity.

V-G Probing Time-Dependent Processes in Solution with Time-Resolved Spectroscopic Methods

Typical molecules in solutions experience several "collisions" in 1 ps. Therefore, many time-dependent processes in solution reach the stationary states in a picosecond time scale. Time-resolved spectroscopic techniques that can record rapidly changing phenomena with a picosecond (10^{-12} s) to sub-picosecond (10^{-13} s) temporal window are effective for probing the time-dependent processes. By using picosecond or femtosecond time-resolved spectroscopic methods, we study the rapidly changing events in solutions. In particular, we try to observe the relative translational motions and the process of intermolecular energy transfer. These processes are deeply involved in the mechanism of a chemical reaction and can determine the fate of the reactant molecules.

We started a new research project for studying the dynamic processes accompanying chemical reactions in solutions with experimental methods. For this purpose, we construct a new time-resolved spectrometer that can trace reaction kinetics in solution with a time resolution of a few hundreds of femtoseconds. With this apparatus, we try to detect time dependent transient absorption associated with electron- or charge-transfer processes, in the near-infrared region. A mode-locked Ti:sapphire laser system modified by Prof. Taira's Group, Laser Research Center for Molecular Science, is used for this study. We also study ultrafast bimolecular reaction kinetics in collaboration with Prof. Tahara's Group. Their femtosecond time-resolved fluorescence spectrometer is successfully applied for tracing ultrafast photochemical reaction between biphenyl and carbon tetrachloride.

V-G-1 Photochemical Bimolecular Reaction between Biphenyl and Carbon Tetrachloride: Observed Ultrafast Kinetics and Diffusion-Controlled Reaction Model

IWATA, Koichi¹; TAKEUCHI, Satoshi; TAHARA, Tahei
(¹IMS and Univ. Tokyo)

[*Chem. Phys. Lett.* **347**, 331 (2001)]

Reaction kinetics of an ultrafast bimolecular reaction is successfully interpreted by theories of diffusion-controlled reactions. When biphenyl is photoexcited to the first excited singlet (S_1) state in carbon tetrachloride solutions, it reacts with the solvent carbon tetrachloride in a few picoseconds. We observe this fluorescence quenching kinetics by using a fluorescence up-conversion technique with a cross correlation time of 320 fs. The obtained decay kinetics is well explained by a model function derived from Smoluchowski's theory of diffusion-controlled reactions when the fitting parameter R , distance between the reactants for the reaction, is 0.39 nm (Figure 1). A modified kinetic theory by Collins and Kimball also gives a satisfactory fit, when R is 0.40 nm and the bimolecular reaction rate constant k_{act} is $3.4 \times 10^{11} \text{ dm}^3\text{mol}^{-1}\text{s}^{-1}$. It is suggested that molecular motions in solution for a time period of a few picoseconds is well described by a concept of diffusion.

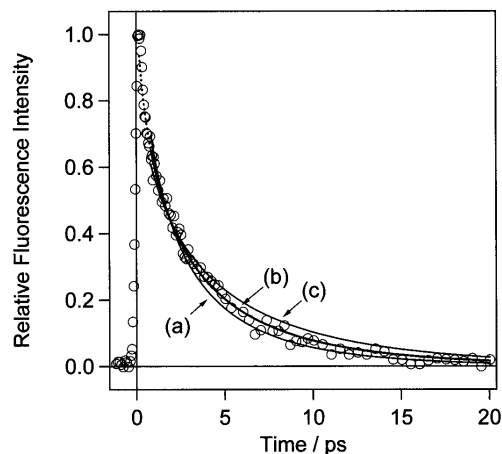


Figure 1. Fluorescence decay curves of biphenyl in carbon tetrachloride simulated by Smoluchowski's theory with the fitting parameter $R = 0.43$ nm (curve (a)), $R = 0.39$ nm (curve (b), best fit), and $R = 0.35$ nm (curve (c)). Observed fluorescence decay curve is also shown with open circles.

V-G-2 Construction of Femtosecond Time-resolved Near-infrared Absorption Apparatus for Tracing Chemical Reaction Dynamics

IWATA, Koichi¹; KURIMURA, Sunao; TAIRA, Takunori
(¹IMS and Univ. Tokyo)

It has been known that some molecular systems show strong electronic transitions associated with electron- or charge-transfer processes in the near-infrared region. Combination or overtone transitions of vibrational levels in general are also located in this spectral region. Therefore, ultrafast time-resolved near-infrared spectroscopy will be quite effective for studying kinetic processes in solution. It provides us with information, on time-dependent phenomena, that is not accessible by other spectroscopic methods. To the best of our knowledge, however, ultrafast time-resolved

near-infrared spectroscopy has been rarely used for studying chemical systems.

We are constructing a femtosecond time-resolved near-infrared absorption apparatus. The apparatus adopts a basic pump-probe scheme. Output light from a mode-locked Ti:sapphire laser (wavelength, 1030 nm; pulse width, 100 fs) is used as “probe” while its second harmonic (515 nm) is used as “pump.” The probe light after the sample is detected with an electrically cooled InGaAs photodiode. Time delay between the pump and probe is controlled by an optical delay unit. We are planning to use the apparatus for tracing kinetics of electron- or charge-transfer reactions.

V-H Stereodynamics of Chemical Reactions and Photodissociation Dynamics

Ionization by metastable atoms (Penning ionization) consists of a spontaneous ionization of the intermediate collisional complex, therefore is a process of fundamental interest behind its importance in plasma and astrochemistry. It has been demonstrated that Penning ionization probes the electron density distribution of the orbital from where the electron is removed, and the collision energy dependence of the ionization cross section has been suggested to be a good measure to clarify anisotropy of intermolecular forces. The reactivity depends not only on the anisotropy of the coupling matrix of $\Gamma = \langle \phi_i | \Phi_{3p} \rangle$, but also on the collision dynamics *via* stereo-anisotropic intermolecular forces, where ϕ_i is the ionized molecular orbital and Φ_{3p} is the atomic orbital of a metastable rare gas. Therefore we study how such steric effect depends on collision energy, as well as on mutual orientation of reactants.

Photo-initiated reaction of weakly hydrogen bonded halide dimer, $(HX)_2$, has a basic potentiality to produce $[XHX]$ transient species by means of the hydrogen atom elimination from $(HX)_2$ dimer. By measuring translational energy distribution of the eliminated hydrogen atom, one can extract information about van der Waals interaction of reactants in the $X + HX$ reaction system. We study the 243-nm photo-dissociation of the DCl clusters by using a Doppler-selected TOF (DS-TOF) technique in order to detect $[ClDCl]$ transient species. We employed the hexapole method to select only the DCl dimer in cluster beam and to exclude any ambiguity about precursor cluster size.

V-H-1 Direct Measurement of Oscillating Behavior in $Ar(^3P) + CH_3Cl \rightarrow Ar + CH_3Cl^+ + e^-$ Ionization Cross Section by Velocity and Orientational Angle Selected Collisions

OHOYAMA, Hiroshi¹; YAMATO, Masanori¹; OKADA, Seiki¹; KASAI, Toshio^{1,2}; BRUNETTI, Brunetto G.³; VECCHIOCATTIVI, Franco³
(¹Osaka Univ.; ²IMS; ³Univ. Perugia)

[*Phys. Chem. Chem. Phys.* **3**, 3598 (2001)]

Collision energy dependence of the ionization cross section for the $Ar(^3P) + CH_3Cl \rightarrow Ar + CH_3Cl^+ + e^-$ reaction was determined under specific relative orientation using an oriented CH_3Cl beam and time-of-flight measurements. A remarkable resonance-type structure is revealed in the energy dependence of orientation angle-resolved Penning ionization cross section. This novel resonance-type structure in Penning ionization cross section could be interpreted as a new-type "nuclear-excited Feshbach resonance" in the formation of vibrational excited Rydberg states leading to a competitive dissociative exit channel.

V-H-2 2D-Measurement of Penning Ionization Cross Section upon Molecular Orientation and Collision Energy in $Ar(^3P_{2,0}) + CHCl_3$ Crossed Beam Reaction

YAMATO, Masanori¹; OHOYAMA, Hiroshi¹; KASAI, Toshio^{1,2}
(¹Osaka Univ.; ²IMS)

[*J. Phys. Chem.* **105**, 2967 (2001)]

The Penning ionization cross section of $Ar^* + CHCl_3$ crossed beam reaction is determined as the function of both molecular orientation and relative collision energy using $CHCl_3$ oriented molecular beam. We find that, the steric opacity function at low collision energies is well correlated to the exterior electron density distribution of $CHCl_3$ molecular orbital which

plays a key role in the electron exchange. At high collision energies, however, the reactivity along the molecular axis is favorable while the sideways approach is found to be unfavorable. The result of our *ab initio* calculation reveals that the collision energy dependence if specified at the sideways shows clear discrepancy with the generally accepted propensity rule based on the type of interaction potential. We propose here that this discrepancy can be ascribed to the collision energy dependent competition of product branching between Penning ionization and neutral dissociation.

V-H-3 Velocity Dependence of the Ionization Cross Section of Methyl Chloride Molecules Ionized by Metastable Argon Atoms

BRUNETTI, Brunetto G.¹; CANDORI, P.¹; FALCINELLI, S.¹; KASAI, Toshio^{2,3}; OHOYAMA, Hiroshi²; VECCHIOCATTIVI, Franco¹
(¹Univ. Perugia; ²Osaka Univ.; ³IMS)

[*Chem. Phys. Phys. Chem.* **3**, 807 (2001)]

The ionization of methyl chloride molecules by metastable argon atom collisions is studied in a crossed beam experiment. The relative cross sections exhibit a decreasing trend in the investigated collision energy range, 0.04–0.3 eV. The results have been analyzed in terms of the potential energy interaction between the two colliding partners, using the optical potential mode. The effect of potential energy anisotropy has also been investigated by the use of a simple sudden approximation within the semiclassical framework. The experimental cross-sections appear to be rather well reproduced by the theoretical calculation with a spherically average potential and very close to the calculation performed using the potential for a perpendicular orientation between the C–Cl axis and the approaching direction of the excited atom.

V-H-4 Photodissociation of DCI Dimer Selected by an Electrostatic Hexapole Field Combined with Doppler-Selected TOF Technique: Observation of [CIDCI] Transient Species

CHE, Dock-Chil; HASHINOKUCHI, Mitihiro¹; SHIMIZU, Yuichiro; KASAI, Toshio¹
(¹IMS and Osaka Univ.)

[*Phys. Chem. Chem. Phys.* **3**, 4979 (2001)]

The photodissociation of DCI dimer, which is preferentially selected from the cluster beam using a hexapole electrostatic field prior to the photolysis, has been studied by a Doppler-selected time-of-flight (DS-TOF) technique at 243 nm. We observed the [CIDCI] transient species through the hydrogen atom elimination from (DCI)₂. By measuring the dependence of the enhancement for the photodissociated D-atom signal upon the hexapole voltage, we find that the DS-TOF spectrum exhibits two kinds of velocity components; one is fast velocity component which originates from only dimer photodissociation, and the other is slow velocity component which originates from not only dimer but also higher sizes of the DCI clusters. For the fast velocity component, the observed spectrum shows an oscillating structure, which could reflect a footprint of nascent internal states (mainly vibration) of the [CIDCI] transient species. The spacing of the observed peaks is about 1000 cm⁻¹, which is much smaller than that of the normal stretching frequency (2091 cm⁻¹) of

the DCI monomer. This result suggests that the observed spectrum reflects the strong perturbation from the Cl atom in [CIDCI].

V-H-5 A New Channel of Hydrogen Elimination in the 121.6-nm Photodissociation of Formic Acid Detected by a Doppler-Selected TOF Mass Spectrometry

HASHINOKUCHI, Mitihiro¹; KOUMURA, Ryouji; CHE, Dock-Chil; KASAI, Toshio¹
(¹IMS and Osaka Univ.)

[submitted for publication]

The 121.6-nm photodissociation of formic acid was investigated by a Doppler-Selected TOF mass spectrometry (DS-TOF-MS) that enables us to map out 3D velocity distributions of photodissociated products through REMPI for the H atoms. The main channel is found to be the HCOO* formation. A new channel of H + CO + OH(X) hydrogen elimination reaction is observed. We estimate that the branching ratio to [H + HCOO*] with respect to [H + CO + OH(X)] is ~5 and those to HCOO(X), HOCO(X) and [2H + CO₂] formation channels are very small. These results show that the DS-TOF-MS method is useful to determine branching ratios and internal energy distributions of photodissociated products in both excited and ground states.

V-I Structure Determination of Neural Clusters

Over the past two decades, much attention has been paid to molecular clusters interfacing material between the gas phase and the condensed phase, from which network interactions could be analyzed at molecular level. Various spectroscopic techniques have been applied to newly synthesized clusters in order to obtain information about energetics, structures and dynamics. Bonding character and structure of clusters are usually reconstructed or modified from its constituent free molecules. Metal-ligand complexes could be treated as small sizes of clusters. Such small clusters serve as a model system for clarifying metal-ligand interaction.

we demonstrate a novel application of the electrostatic hexapole field to the supersonic beams of Al-CH₃CN and Al-NH₃ synthesized complexes for the determination of permanent dipole moments, which are relevant to the nature of dipole-induced dipole and dipole-dipole interactions between the metal atom and the ligand molecule. Second, in an attempt to clarify the weak interaction and the bonding nature between the Al atom and C₆H₆, we selected Al(C₆H₆) isomers and determined the dipole moments using the 2-meter electrostatic hexapole. We have also performed the density functional calculations (DFT) of the isomers at B3LYP/6-31G* level for obtaining geometries and electric features of the isomers.

V-I-1 Non-Destructive Selection of Geometrical Isomers of Al(C₆H₆) Cluster by a 2-Meter Electrostatic Hexapole Field

IMURA, Kohei¹; KAWASHIMA, Takahiro¹; OHYAMA, Hiroshi¹; KASAI, Toshio^{1,2}; NAKASHIMA, Atsushi³; KAYA, Koji
(¹Osaka Univ.; ²IMS; ³Keio Univ.)

[*Phys. Chem. Chem. Phys.* **3**, 3593 (2001)]

A supersonic cluster beam which contains isomers of Al(C₆H₆) complexes is generated by a laser evaporation, and the cluster is non-destructively selected using a 2-meter-long electrostatic hexapole. The focusing curve shows clear evidence that there are two kinds of Al(C₆H₆) isomers which are slightly different from each other in geometry; namely one is an asymmetric 1,2-complex and the other one is a nearly C_{6v} symmetric 1,4-complex. The electric dipole moments of the two isomers are found to be 1.5 ± 0.1 and 1.4 ± 0.1 D, respectively. We carried out

computation using the density functional theory in order to estimate their structures. We find that the 1,2-complex is more stable than the 1,4-complex. The present work confirms that the electrostatic hexapole technique is useful for non-destructive selection of the geometrical isomers in the beam.

V-I-2 Direct Determination of the Permanent Dipole Moments and Structures of Al-CH₃CN and Al-NH₃ by Using 2-Meter Electrostatic Hexapole Field

**IMURA, Kohei^{1,2}; KAWASHIMA, Takahiro¹;
OHOYAMA, Hiroshi¹; KASAI, Toshio^{1,2}**
(¹Osaka Univ.; ²IMS)

[*J. Am. Chem. Soc.* **123**, 6367 (2001)]

The supersonic beams of pure metal-ligand (1-1) complexes of Al-CH₃CN and Al-NH₃ were synthesized by a laser evaporation flow-tube-reactor method and non-destructively structure-selected by a 2-meter long electrostatic hexapole field. The permanent dipole moments of such selected complexes were determined. We find that the competing effects of "charge transfer" and "polarization" through the metal-ligand bond can be estimated by measuring the change in the magnitude of permanent dipole moments before and after the complex formation of Al-CH₃CN and Al-NH₃. The *ab initio* calculation at the MP2 level was performed in order to simulate the complex structures and to explain the experimental findings.

V-J Monte Carlo Simulation of Molecular Clusters

Monte Carlo simulation is a powerful method for studying soft matter such as polymer and gel. We performed the structure analysis of chemical gel and characterized gel with cross-linkers. For DNA in polymer solution, we simulated the linear-shaped and U-shaped motion, and studied the conditions for such motions. In both systems, we obtained qualitatively good agreement with experimental results.

V-J-1 Structure Analysis of Chemical Gel Using Monte Carlo Simulation

NOSAKA, Makoto; TAKASU, Masako

[*Trans. Mater. Res. Soc. Jpn.* **26**, 557 (2001)]

We studied the structure of gel using Monte Carlo simulation with modeled radical reactions. Simulation is performed using beads-spring model in three-dimensional continuous space. For the criterion of gel, we apply the concept of percolation to our clusters; we calculate the maximum size in all directions for each cluster, and sum up the number of percolated direction for all percolated clusters in a system. We call this the number of percolation. We obtained structure information of system from plotting the average number of percolation. We can determine whether the system has percolated clusters, and also whether the polymer network has inhomogeneous structure.

V-J-2 Characterization of Gel Using Modeled Radical Polymerization with Cross Linkers Performed by Monte Carlo Method

NOSAKA, Makoto; TAKASU, Masako; KATOH, Kouichi¹

(¹Kanazawa Univ.)

[*J. Chem. Phys.* submitted]

In this study, some physical quantities for characterization of gel are proposed. Polymer networks (gel) are investigated by Monte Carlo simulation using modeled free-radical cross-linked polymerization in continuous system. The distributions of degree of polymerization for clusters obtained in this simulation show qualitatively good agreement with the experimental results. Linkers are classified to two types according to the roles in networks, and their ratios are discussed. The normal and weighted ratios of gel are defined using percolation theory. These ratios are compared with the changes in distribution.

V-J-3 Linear-Shaped Motion of DNA in Entangled Polymer Solutions under a Steady Field

NOGUCHI, Hiroshi; TAKASU, Masako

[*J. Phys. Soc. Jpn.* **69**, 3792 (2000)]

We studied the electrophoretic behavior of DNA chains in linear-polymer solutions using Brownian dynamics with an anisotropic friction tensor. We

simulated the linear-shaped motion of DNA observed in highly entangled solutions (Ueda *et al.*) using a model with a chain segment equal to 1/4 of the persistence length. A linear conformation is seen for a chain with high segment-density regions, which remain at the same positions in space, with a high anisotropy of friction, while a U-shaped conformation is seen for a chain with a low anisotropy of friction.

V-J-4 Dynamics of DNA in Entangled Polymer Solutions: An Anisotropic Friction Model

NOGUCHI, Hiroshi; TAKASU, Masako

[*J. Chem. Phys.* **114**, 7260 (2001)]

We studied the electrophoretic behavior of DNA chains in linear-polymer solutions using Brownian dynamics with an anisotropic friction model in a three-dimensional space and projected on x-axis. For the three-dimensional model with a chain segment equal to 1/8 of the Kuhn length, a chain migrates with U-shaped conformation with low anisotropy of friction. With high anisotropy of friction, a chain always migrates with linear-shaped conformation with high segment-density regions, which remain at the same positions in space. This migration mode agrees with the observation of DNA in highly entangled solutions. [Ueda *et al.*] The projection model also reproduces the linear-shaped motion. We clarified that the essential conditions for linear shaped motion are the sufficient chain length of DNA, the small mesh size, and strong confinement by entanglement with solvent polymers.

V-J-5 Electrostatic Behavior of Polyelectrolytes in Gel and Polymer Solutions

NOGUCHI, Hiroshi

[*Trans. Mater. Res. Soc. Jpn.* **26**, 687 (2001)]

Electrophoresis using gel and uncrosslinked polymer solutions is widely used to separate DNA chains by chain length. We studied the electrophoretic behavior of chains using Brownian dynamics with an anisotropic friction tensor. We show the anisotropic-friction model proposed by Curtiss and Bird is an effective method to describe dynamics of polyelectrolyte chains under an electric field in gel and polymer solutions. With a low anisotropy of friction (dilute polymer solutions), a chain fluctuates between elongated and compact states with no periodicity under a steady electric field. On the other hand, with a high anisotropy of friction (gel or entangled polymer solutions), a chain oscillates periodically: Polyelectrolyte chain is trapped by gel fibers with a U-

shaped conformation, stretches out, and re-acquires a compact conformation. The above results agree well with experiments on DNA electrophoresis.

V-K Development of Broadband Solid-State NMR Spectroscopy

Ordinary NMR probes employ resonant circuits, which can be tuned only over a bandwidth of a few 100 kHz. Most of the NMR probes have been well developed and are commercially available, although they are very expensive. However, solid samples often have much larger line widths than the bandwidth of the resonant probe. Such examples are many of quadrupole nuclei (examples Cl, Br, I, Nb *etc.*) and metal nuclei (Pt, Rh, Hg, Pb *etc.*) having large Knight shifts. The samples containing these nuclei have been studied by rather simple methods as Hahn echo measurements or relaxation measurements by irradiating only a part of the spectral region. The whole spectra is obtained either by changing the static magnetic field or by changing the carrier frequency and probe tuning. Only in a few cases, more than one carrier frequency was employed to correlate different spectral regions.^{1,2)} A broadband NMR probe that does not use the resonant circuits may be necessary to conduct two-dimensional NMR experiments or automated experiments over the whole spectral range. Lowe and coworkers proposed a transmission line NMR probe in the 70s and it is expected to have much larger bandwidth than a normal resonant circuit.^{3,4)} In our study we reexamined the transmission line probe by numerical simulations and experiments.

References

- 1) J. Haase, M. S. Conradi, C. P. Grey and A. J. Vega, *J. Magn. Reson. A* **109**, 90 (1994).
- 2) J. Haase, N. J. Curro and C. P. Slichter, *J. Magn. Reson.* **135**, 273 (1998).
- 3) I. J. Lowe and M. Engelsberg, *Rev. Sci. Instrum.* **45**, 631 (1974).
- 4) I. J. Lowe and D. W. Whitson, *Rev. Sci. Instrum.* **48**, 268 (1977).

V-K-1 Numerical Simulations of the Transmission Line Probe

KUBO, Atsushi; ICHIKAWA, Shinji

The transmission line probe resembles a circuit of a low-pass filter, which consists of π sections with a coil and two capacitors, which connect the ends of the coil to ground. To simulate the real transmission line probe, we need to include the inductive coupling between all the coils in the different π sections, which was taken into account as a parameter in the Lowe's analyses. In our analysis, we calculated the self and mutual inductance explicitly by using the Neumann's formula. The method of the simulation is based on the moment method.¹⁾ We calculated the effective impedance, the propagation constants and the scattering matrix, which characterize the probe circuit.²⁾ We also calculated the strength of the rotating magnetic field as a function of carrier frequency and position. It is interesting to note that the scattering matrix is also employed in other fields as conductance of carbon nanotubes and an optical resonator.

We compared our numerical results with the analytical equations derived by Lowe. We found that their equations agree well with our numerical results, if the self-inductance of the low-pass filter was replaced by the average inductance, which is defined as the total inductance divided by the number of π sections. We considered a rectangular flat coil with a pitch p , wire length $l \gg d$ (d is the length along the static magnetic field), number of turns N_i and cable impedance Z_0 . We modified one of Lowe's equations and found that the rotating field at the coil center becomes an exponentially decaying function of carrier frequency ν ,

$$|B_+| = (\mu_0 V_{in} / 2Z_0 p) \exp(-\nu/\nu_d),$$

where $\nu_d = (2Z_0 / \pi \mu_0 l)(p/d)^2$ and V_{in} is the input voltage.

To obtain a large RF field, the pitch of the coil or the impedance of the probe must be small. The latter need the impedance transformation from the cable impedance of 50Ω . The above equation also requires that ν_d must be much larger than the observed frequency, which restricts the dimensions of the coil.

We also found that the reflection of waves takes place near both ends of the coil. Since the coil near the ends has only one neighbor, its total inductance is smaller than that at the center. The reflection causes the undulation of the magnitudes of currents over different π sections and also the undulation of the field strength, thus spoiling the homogeneity of the magnetic field. We could also see the effect of diffraction at the carrier frequencies where the phase delay through the probe becomes close to integer multiples of π . Near these frequencies, the effective impedance showed a dispersion curve and the propagation constant became real positive, which means that the circuit absorbed energy. Next we varied the pitch of the coil and made it smaller near both ends. This treatment suppressed the undulation of currents and thus improved the homogeneity of the RF field in the coil.

References

- 1) M. N. O. Sadiku, "Numerical Techniques in Electromagnetics," CRC Press; Boca (2001).
- 2) S. Ramo, J. R. Whinnery and T. Van Duzer, "Fields and Waves in Communication Electronics," Wiley; New York, (1994).